



Effects of melt treatment temperature and isothermal holding parameter on water-quenched microstructures of A356 aluminum alloy semisolid slurry

Ming LI¹, Yuan-dong LI^{1,2}, Guang-li BI^{1,2}, Xiao-feng HUANG^{1,2}, Ti-jun CHEN^{1,2}, Ying MA^{1,2}

1. State Key Laboratory of Advanced Processing and Recycling of Nonferrous Metals, Lanzhou University of Technology, Lanzhou 730050, China;
2. Key Laboratory of Nonferrous Metal Alloys and Processing, Ministry of Education, Lanzhou University of Technology, Lanzhou 730050, China

Received 19 September 2016; accepted 4 December 2017

Abstract: The semisolid slurry of the A356 aluminum alloy was prepared by self-inoculation method (SIM), the effects of melt treatment temperatures and isothermal holding parameters on water-quenched microstructures of A356 aluminum alloy semisolid slurry were investigated, and the solidification behavior of the remaining liquid phase (secondary solidification) was analyzed. The results indicate that the melt treatment temperature has significant effects on the final semisolid microstructures. The semisolid slurry which is suitable for the rheological forming can be produced when the melt treatment temperature is between 680 and 690 °C. During the isothermal holding process, the growth rate of the primary particles conforms to the dynamic equation of $D_t^3 - D_0^3 = Kt$, and the coarsening rate of the primary particles is the fastest when the isothermal holding temperature is 600 °C. Additionally, the isothermal holding time also has obvious effect on the secondary solidification microstructures. The secondary particles are the smallest and roundest when the isothermal holding time is 3 min. The amount of the secondary particles gradually increases with the increase of isothermal holding temperature, and the eutectic reaction therefore is confined into small intergranular areas, contributing to the compactness of the final solidified eutectic structures.

Key words: aluminum alloy; semisolid; self-inoculation method; secondary solidification; primary particles; eutectic structure

1 Introduction

As the demands for high performance, high reliability and lightweight components are more and more urgent due to the increasing pressure of energy saving and emission reduction during the environmental protecting, the development of advanced forming theory, method and technology with proprietary intellectual property rights has been paid much attention to the automotive industry and the new technology fields [1]. Compared with high pressure casting, vacuum die casting and squeeze casting, semisolid rheological forming technology is a more promising technology capable of producing high-integrity components, and the utilization rate of material property is higher than that of the same kind of casting parts. The quality utilization rates of rheological forming materials are close to those of high pressure casting materials. Meanwhile, semisolid

rheological forming technology can not only form complex-shaped components, but also reduce the forming equipment tonnage and energy consumption [2–6]. Therefore, rheological forming is regarded as one of the most promising forming technologies of metal materials in the 21st century.

Slurry preparation process is a key step in the development of the rheological forming technology. In recent years, a variety of semisolid slurry preparation technologies have been proposed, such as the twin-screw slurry maker [7], GISS (gas induced semisolid) [8], SCP (serpentine pouring channel) [9], WSP (wavelike sloping plate) [10], SSR (semi-solid rheocasting) [11], CRP (continuous rheoconversion process) [12], NRC (new rheocasting process) [13], and SEED (swirled enthalpy equilibration device) [14].

The solidification process of semisolid metal forming can be divided into two stages: the stage of slurry preparation (solid particles crystallize from the

liquid alloy) is called primary solidification, and the solidification stage of slurry in the forming process (solidification of the remaining liquid) is called secondary solidification [15]. Although the primary solidification has been extensively investigated and comprehensively understood, not much attention has been paid to the solidification of the remaining liquid. Theoretically, the secondary solidification including the crystallization of the secondary primary phase and eutectic reaction, accompanied with the volume shrinkage and segregation problems, results in some defects such as shrinkage, hot cracking and nonuniform microstructure. FAN et al [16–18], REISI and NIROUMAND et al [19], ZANLER et al [20], GUAN et al [21,22] and CHEN et al [23] studied the solidification microstructures of the remaining liquid phase of different alloys using different methods, and indicated that the slurry preparation process, solid phase fraction and cooling rate have significant effects on the solidification behavior of the remaining liquid and its microstructures.

Hence, in order to promote the application of semisolid rheological forming technology, it is necessary to study the influence of processing parameters and solid fraction during the process of slurry preparation on the solidification behavior of the remaining liquid phase. In the present work, semisolid slurry of the A356 aluminum alloy was prepared by self-inoculation method (SIM) [24]. The effects of melt treatment temperature and isothermal holding parameters on microstructures of the A356 aluminum alloy (microstructures of primary solidification and secondary solidification) were studied to provide a theoretic basis for the optimization of processing parameters and its application.

2 Experimental

Figure 1 shows the schematic diagram of slurry preparation by SIM [15]. The fluid director was inclined at 45° with a length of 500 mm. The commercial A356 alloy (composition as shown in Table 1) was melted in a pit-type electric resistance furnace and degassed by C_2Cl_6 (1% of the alloy mass) when the melt temperature reached 720 °C, the melt temperature was adjusted to 700, 690, 680 and 670 °C, respectively, and then self-inoculants (5% of alloy mass, with the size of 5 mm×5 mm×5 mm) were added into the melt and stirred with iron bars quickly. After that, the mixed melt was collected through fluid director to the slurry collector to gain semisolid slurry, and directly poured into cold water to obtain water-quenched specimens without isothermal holding. Finally, the prepared slurry was isothermally held for a certain time (3, 5 and 10 min) at different holding temperatures (610, 600 and

590 °C), and then directly poured into cold water to obtain water-quenched specimens with different isothermal holding parameters.

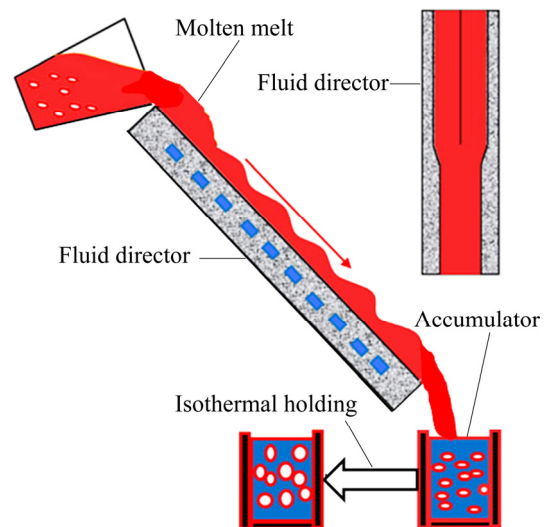


Fig. 1 Schematic diagram of slurry preparation by SIM [15]

Table 1 Chemical composition of commercial A356 alloy (mass fraction, %) [15]

Si	Mg	Fe	Ti	Cu	Zn	Al
7.06	0.27	0.115	0.097	0.001	0.01	Bal.

Specimens were prepared by the standard technique of grinding with SiC abrasive paper and polishing with an Al_2O_3 suspension solution, followed by etching in saturated NaOH aqueous solution. The microstructures of the specimens were observed by an MEF-3 optical microscopy (OM). The average particle size ($D=(4A/\pi)^{1/2}$, where A is the area of the particle) and shape factor ($F=P^2/(4\pi A)$, where P is the perimeter of particle) of the primary particles, were measured using image analysis software Image-Pro Plus 5.0. The FEG450 scanning electron microscopy (SEM) observation was carried out in an energy dispersive spectroscopy (EDS) facility and was operated at an accelerating voltage of 3–20 kV to observe the morphologies of the secondary particles and eutectic structures [15].

Figure 2 shows the schematic diagram of the temperature change in the SIM process. When the melt temperature reaches T_1 , the self-inoculants are added and the temperature is reduced to T_2 . And then the temperature is reduced to T_3 after the melt flows through the fluid director, and there is an isothermal holding process for a specific time at temperature of T_3 . Finally, the forming process is carried out. In this experiment, the average temperature reduction (T_2-T_1) after adding self-inoculants is about 50 °C, and the temperature drops about 30 °C (T_3-T_2) after the melt flows through the fluid director. Thus, the mean temperature change in the

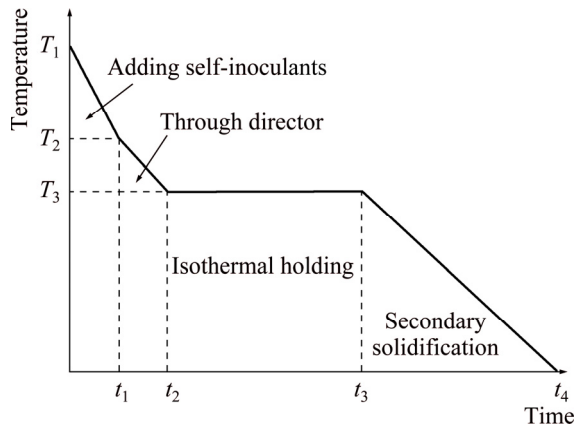


Fig. 2 Schematic diagram of temperature change in semisolid process by SIM

whole process of SIM is reduced by about 80 °C, which can be used as a reference value for presetting holding temperatures of different melt treatment conditions. Therefore, the setting value of the heat preservation temperature in this experiment is 80 °C below the melt treatment temperature.

3 Results and discussion

3.1 Effects of melt treatment temperature on water-quenched microstructures

Figure 3 shows the water-quenched microstructures of the A356 aluminum alloy prepared by SIM at different melt treatment temperatures. It can be seen that the

amount of the primary particles gradually decreases when the melt treatment temperature increases from 670 °C (Fig. 3(a)) to 690 °C (Fig. 3(c)). When the melt treatment temperature is 700 °C, after being treated by SIM, there is no primary solid particle in the water-quenched microstructure (Fig. 3(d)). Therefore, it can be seen that the melt treatment temperature has great effects on water-quenched microstructures of the A356 aluminum alloy semisolid slurry when the angle of the fluid director and the addition amount of self-inoculants are certain.

According to the melting model of the self-inoculants [25], the melting state of self-inoculants can be expressed by the solid fraction f_s :

$$f_s = \frac{T - T_L}{T_S - T_L} \quad (1)$$

where T_S is the solidus temperature of the alloy, and T_L is the liquidus temperature of the alloy.

The temperature of the self-inoculants at the outlet of the fluid director (T) is linear with temperature change of the melt (ΔT):

$$T = k\Delta T + b \quad (2)$$

In this equation,

$$k = \frac{(100/x)(T_S - T_L)c_p}{c_p(T_S - T_L) - L}; \quad b = \frac{c_p T_r (T_S - T_L) - L T_S}{c_p(T_S - T_L) - L}$$

where c_p is the specific heat capacity of the alloy, x is the addition amount of the self-inoculants, T_r is the room

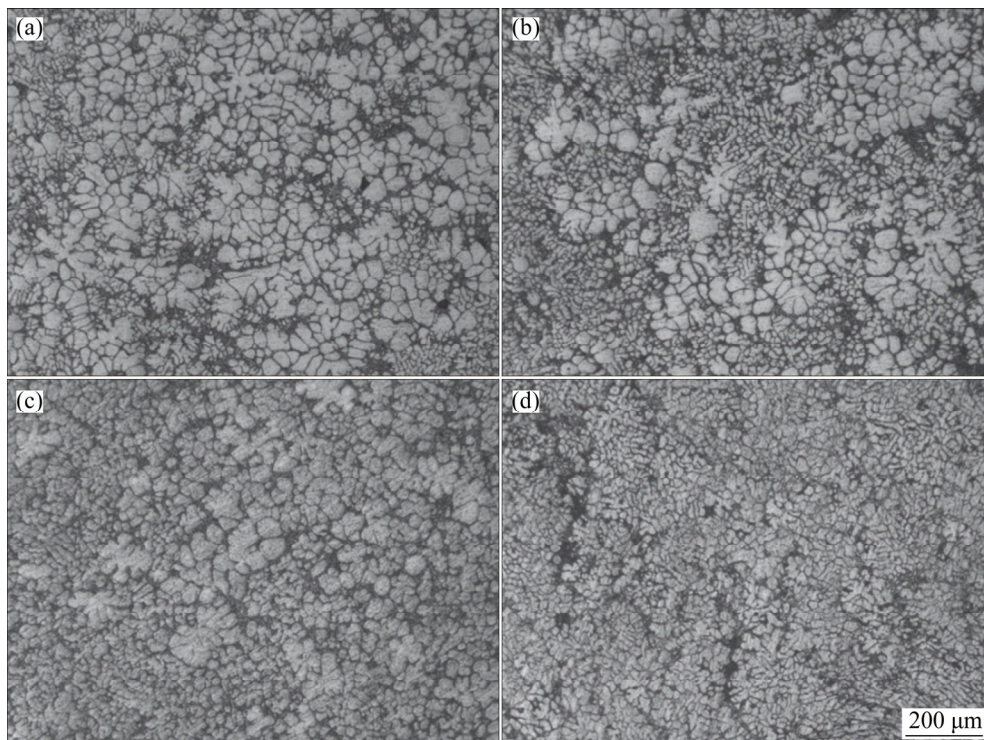


Fig. 3 Water-quenched microstructures of A356 aluminum alloy prepared by SIM at different melt treatment temperatures: (a) 670 °C; (b) 680 °C; (c) 690 °C; (d) 700 °C

temperature, L is the latent heat. Due to the minimum value of solid fraction is 0, Eq. (1) is defined as follows: if the temperature of the self-inoculants at the outlet of the fluid director (T) is higher than the liquidus temperature of alloy (T_L), f_s equals 0.

Thermal physical values of the A356 aluminum alloy are shown in Table 2. And Table 3 shows the measured temperatures of the A356 aluminum alloy during the process of SIM, where T_t is the melt treatment temperature, T_{in} is the temperature at the inlet of the fluid director, and T_{out} is the temperature at the outlet of the fluid director. Substitute the values of the thermal parameters and the measured temperatures into Eq. (2) to obtain the self-inoculants temperatures at the outlet of the fluid director T (as shown in Table 4) and then substitute the obtained temperature values into Eq. (1) to calculate the corresponding solid fraction f_s . After above process, the calculated temperature of self-inoculants at the outlet of the fluid director is 630 °C when the melt treatment temperature is 700 °C, which is higher than the liquidus temperature of the A356 aluminum alloy (615 °C). According to the definition, the solid fraction of the slurry is 0. While the solid fraction f_s is calculated to be 15%, 20% and 35%, corresponding to the melt treatment temperatures of 690, 680 and 670 °C, respectively. Combining with Fig. 3, it can be concluded

Table 2 Thermodynamic data of A356 aluminum alloy

x	T_S/K	T_L/K	T_f/K	$c_p/(J \cdot mol^{-1} \cdot K^{-1})$	$L/(J \cdot mol^{-1})$
5	828	888	293	35.7	12781

Table 3 Temperature variation of A356 aluminum alloy during SIM process

$T_t/°C$	$T_{in}/°C$	$T_{out}/°C$	$\Delta T/°C$	$\Delta T_t/°C$
700	647	615	53	32
690	645	612	45	33
680	640	606	40	34
670	633	605	37	28

$$\Delta T = T_t - T_{in}; \Delta T_t = T_{in} - T_{out}$$

Table 4 Fusional state of self-inoculants of A356 aluminum alloy at different melt treatment temperatures

$T_t/°C$	$T/°C$	$f_s/\%$
700	630	0
690	607	15
680	593	20
670	584	35

that the solid fraction of the slurry decreases with the increase of the melt treatment temperature.

According to the structure hypothesis of the liquid metal [26], the metal melt is made up of atomic clusters and atoms with certain sizes. The cluster can maintain the stability with a certain size and structure under a certain temperature condition. When the temperature decreases, the size and structure of the cluster are changed as shown in Fig. 4 [27]. The change of the melt structure is shown in Fig. 5 [25]. The solid self-inoculants have long range ordered atomic structures, while the liquid melt has short range ordered atomic structure with many high melting point particles (as the black points shown in Fig. 5). After adding the self-inoculants, there will be some small undercooling zones in the melt, and the high melting point particles will bond the nearby atoms, which will lead to the increase of magic amount of atomic cluster. While the atomic clusters and their amount can be affected by the melt treatment temperature. When the melt treatment temperature is too low (670 °C), on one hand, the atoms can combine with high melting point to form large cluster. On the other hand, the self-inoculants are not completely melted and a large amount of clusters are formed, which leads to the large value of f_s in Eq. (1). On the contrary, when the melt treatment temperature is too high (700 °C), clusters are difficult to be formed due to the completely melted self-inoculants. Moreover, less high melting point particles in the melt reduce the formation probability of the nucleus by accumulating atoms with high melting particles, which causes f_s close to 0. When the melt treatment temperature is in a proper temperature range (680–690 °C), two factors play an effective role in the formation of clusters. As a result, the magic amount of clusters is not too large and clusters can be evenly distributed in the melt.

3.2 Effects of isothermal holding parameter on primary particles

The microstructures of the water-quenched A356 aluminum alloy semisolid slurry during isothermal holding process are shown in Fig. 6. It shows that the semisolid slurry containing rose-shape and fine dendritic primary particles can be prepared by SIM (Figs. 6(a)–(c)). After holding for a short time (such as 3 and 5 min), the dendrite arms of the primary particles are fusing, and primary particles become spherical

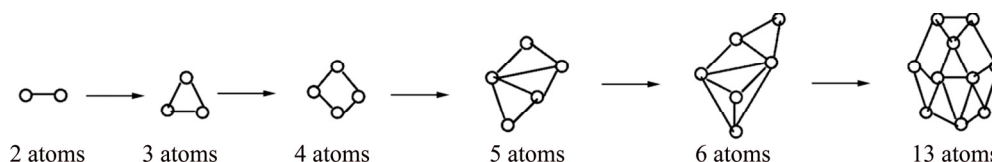


Fig. 4 Structure evolution of atomic cluster during size change [27]

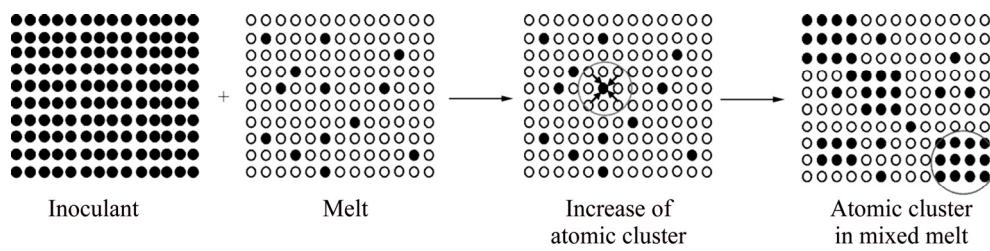


Fig. 5 Schematic diagrams of structures of self-inoculants, melt and mixed melt [25]

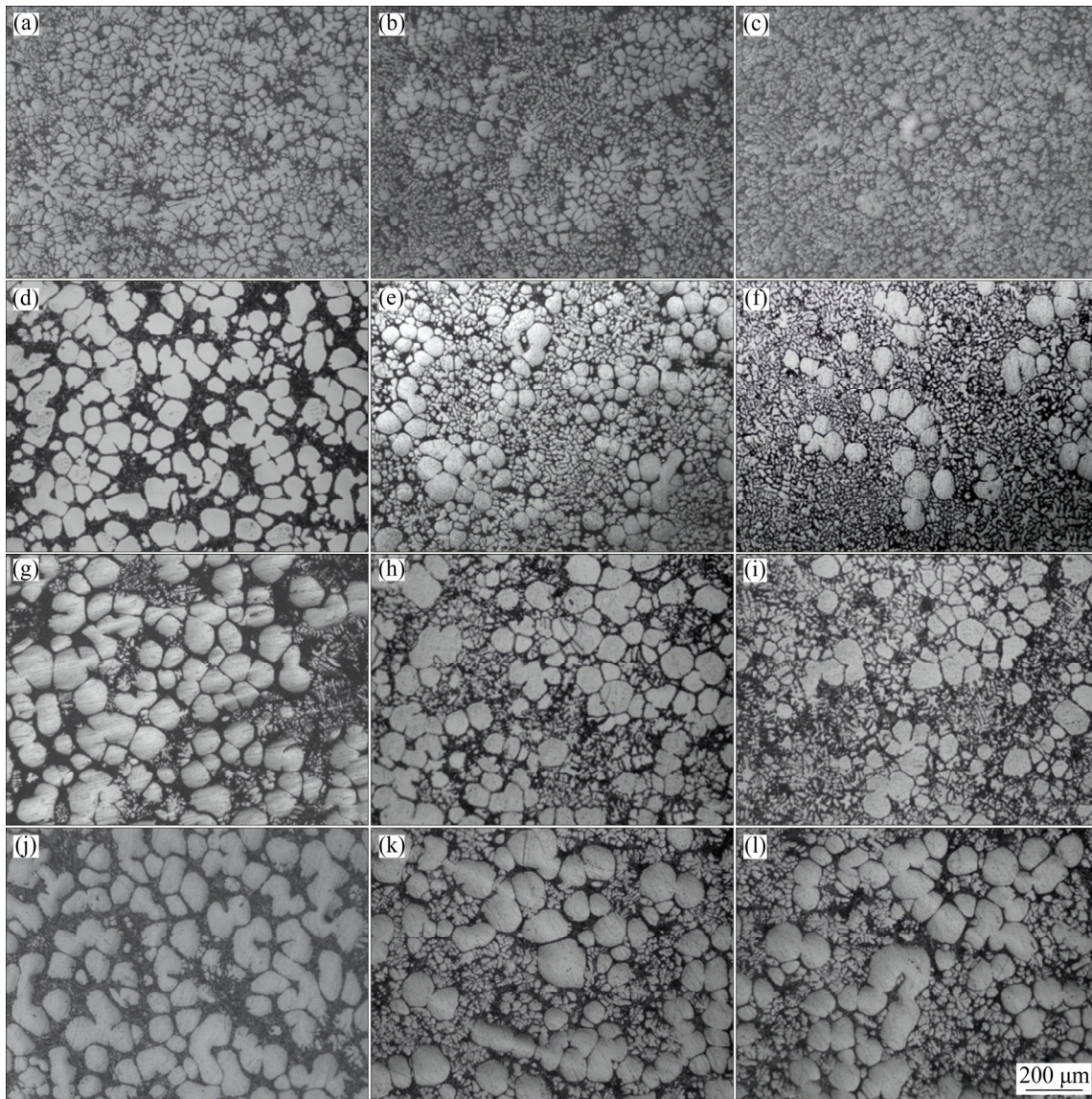


Fig. 6 Microstructures of water-quenched A356 aluminum alloy semisolid slurry after isothermal holding process: (a, d, g, j) Holding at 590 °C for 0, 3, 5 and 10 min, respectively; (b, e, h, k) Holding at 600 °C for 0, 3, 5 and 10 min, respectively; (c, f, i, l) Holding at 610 °C for 0, 3, 5 and 10 min, respectively

(Figs. 6(d)–(f)). But when the holding time of slurry is too long (such as 10 min), the sizes of primary particles increase while the merging phenomenon among primary particles occurs, which leads to the emergency of “8” shape or “spindle-like” structures (Figs. 6(j)–(l)).

The effects of isothermal holding time and

temperature on average particle sizes (Fig. 7(a)) and shape factors (Fig. 7(b)) of the primary particles are measured, as shown in Fig. 7. This illustrates that the primary particle sizes are from 35 to 42 μm when the holding time is 0 min and the melt treatment temperature increases from 590 to 610 °C, but the shape factors are

from 1.8 to 2.0. It should be noted that the average sizes and shape factors of the primary particles are gradually decreasing with the decrease of the melt treatment temperatures. When the isothermal holding time is 3 min, the particle sizes are increased to more than 60 μm and the shape factors are reduced to about 1.4. In addition, the growth rate of the primary particles from 0 to 3 min at 610 °C is lower than that of the other two temperatures. When the holding time is increased to 5 min, the sizes of the primary particles are increased to 70–80 μm. When the holding time is increased to 10 min, the sizes of the primary particles are more than 100 μm, and the shape factors are larger than that at 5 min.

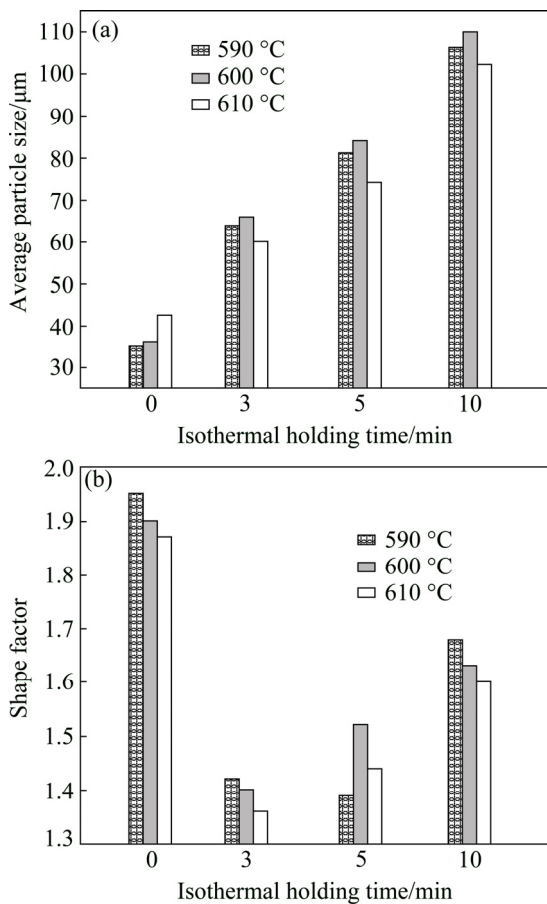


Fig. 7 Effects of isothermal holding time and temperature on average particle size (a) and shape factor (b) of primary particles

Figure 8 shows the linear fitting of the growth of the primary particles with different isothermal holding parameters. It can be seen that the primary particles are gradually growing and spheroidizing in the early stage of isothermal holding process, and the growth rate of the primary particles in the isothermal holding process conforms to the dynamic equation of $D_t^3 - D_0^3 = Kt$ [28] (where D_0 is the initial particle size, D_t is the average particle size after isothermal holding for time t , and K is the coarsening rate constant). After the fitting analysis,

the coarsening rate constant K and the fitting coefficients R^2 are obtained as shown in Table 5. It illustrates that the regression coefficients are close to 1 when the isothermal holding temperatures are 590 and 600 °C, respectively. Meanwhile, it is also visible that the coarsening rate constant K reaches the maximum at 600 °C, while the minimum at 610 °C.

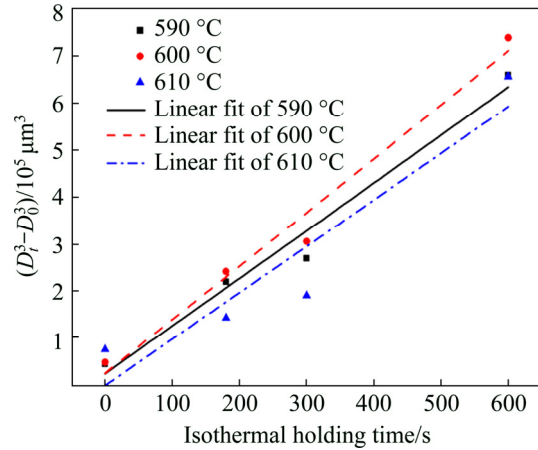


Fig. 8 Linear regression of growth of primary particles

Table 5 Linear fitting data of primary particles growth law of A356 aluminum alloy in isothermal holding stages

Temperature/°C	Theoretical solid fraction, $f_s/\%$	Slope, $K/(\mu\text{m}^3 \cdot \text{s}^{-1})$	$D_0/\mu\text{m}$	Fitting coefficient, R^2
590	37.5	1019.02	35	0.96508
600	27.0	1145.29	36	0.96916
610	11.0	992.53	42	0.84125

When the slurry is prepared without isothermal holding, the measured temperatures of the semisolid slurry are 605 and 606 °C, respectively, corresponding to the melt treatment temperatures of 670 and 680 °C, respectively (as shown in Table 3). Thus, the differences of average sizes and shape factors of the primary particles between the above two temperatures are not obvious. While the slurry temperature is measured to be 612 °C when the melt treatment temperature is 690 °C, which is higher than other two temperatures, causing that the elements diffusion is the fastest in the slurry at 612 °C. Hence, the growth rate of the dendrite fragments is the fastest. However, due to the high temperature of the melt, the sharp of dendrite fragments will be passivated. As a result, the average size of primary particles is the largest while the shape factor is the smallest when the melt treatment temperature is 690 °C. During the isothermal holding process, the dendrite roots are fused due to the solute enrichment, which leads to the formation of single irregular particles. Meanwhile, the increasing amount of particles makes the interfacial energy increased. Primary particles, as the substrates to

absorb solute atoms from liquid phase, are rounded and spherical under the influence of the driving force—the interfacial energy can be reduced as far as possible [15]. Consequently, primary particles are increased and spheroidized with the extension of isothermal holding time. However, different sizes of original dendrite fragments result in different diameters of spherical primary particles after isothermal holding for a short time. The solute concentration of liquid phase around small particles is lower than that around the large particles. With the further extension of the holding time, Si elements will continue to diffuse from large particles to small particles, while the Al elements have the opposite diffusion path. As a result, the large particles become larger and the small particles become smaller even melt and disappear, which is called Oswald ripening [29]. The solid phase diffusion causes the coarsening and spheroidizing of the primary particles in the slurry. However, different solid fractions will also cause different coarsening rates. When the holding time of the slurry is 610 °C, the volume of liquid phase and the primary particles spacing are large, causing the long solute diffusion distance, which leads to the small coarsening rate of the primary particles. On the contrary, when the isothermal holding temperature is 590 °C, the solid fraction of the slurry is high, leading to less liquid phase. Therefore, the ability of the solute diffusion is limited and the coarsening rate is small. When the isothermal holding temperature is 600 °C, both the solid fraction and the primary particles spacing are not large enough, leading to the largest coarsening rate of the primary particles. The “8” shape or “spindle-like” structures are formed as the intensification of merging phenomenon in the late stage of isothermal holding process. When two particles with large difference in size are incorporated and grow into a new shape, the new particle will eventually be spherical under the driving force of the reduced interfacial energy. However, when two particles with the same size are merged into a new particle, it will be very difficult for the resulting particle to be spherical, and it will eventually grow into “8” shaped clusters.

3.3 Effects of isothermal holding parameters on secondary solidification microstructures

Figure 9 shows the secondary solidification microstructures of the A356 aluminum alloy semisolid slurry after water-quenched process with different isothermal holding parameters. It is evident from Fig. 9 that the secondary particles are rose-like and near spherical crystals when the isothermal holding time is 3 min. While the secondary solidification microstructures are mainly equiaxed crystals and even dendrites attaching to primary particles when the holding time is

0 and 5 min, respectively (Fig. 9(g)). When the holding time is increased to 10 min, the attaching growth phenomenon is more prominent, and the dendrites appear in microstructures of all the three temperatures. The average sizes and shape factors of water-quenched secondary particles are tallied, and the changes of sizes and shape factors with isothermal holding time are shown in Fig. 10. In addition to the microstructures without isothermal holding, the secondary particle sizes are gradually increased with the increase of the isothermal holding time (Fig. 10(a)). The secondary particle sizes are the smallest when the isothermal holding time is 3 min. Moreover, the shape factors of secondary particles are the smallest (close to 1) when the isothermal holding time is 3 min. This indicates that the secondary particles are the roundest and smallest after an isothermal holding time of 3 min.

Figure 11 shows the changes of the attached secondary particle sizes with isothermal holding time during water-quenched process. It can be seen that the sizes of secondary particles attached to the primary particles are the smallest when the holding time is 3 min in the condition of three holding temperatures. When the isothermal holding temperature is 600 °C, the sizes of the attached secondary particles are significantly smaller than those of other two temperatures, indicating that the attaching growth phenomenon at 600 °C is the slightest. In addition, it can be further proved by combining Fig. 10 with Fig. 11 that the secondary particles are the roundest and smallest when the slurry is isothermally held at 600 °C for 3 min.

As for the slurry without isothermal holding, there are high temperature regions and forced convections in the slurry due to the inhomogeneous distribution of thermal field and concentration field. When the isothermal holding time is 3 min, the thermal field and concentration field of the slurry are homogeneous, the convection is weakened and high temperature regions gradually disappear. Hence, the average size and shape factor of the secondary particles are smaller than those without isothermal holding. When the isothermal holding time is 5 min, the convection is further reduced, but the thermal field and concentration field in the slurry are inhomogeneous again due to the merging of the primary particles, leading to the temperature fluctuation and the solute diffusion layer formed at local positions. It is not only detrimental to the nucleation of the remaining liquid phase during the water-quenched process, but also promoting the attaching growth of the secondary particles. Thereby, the dendrites which are attached to primary particles are generated, leading to the increase of the shape factors. After a very long holding time (10 min), the convection in the remaining liquid phase completely disappears, and the inhomogeneous degree of

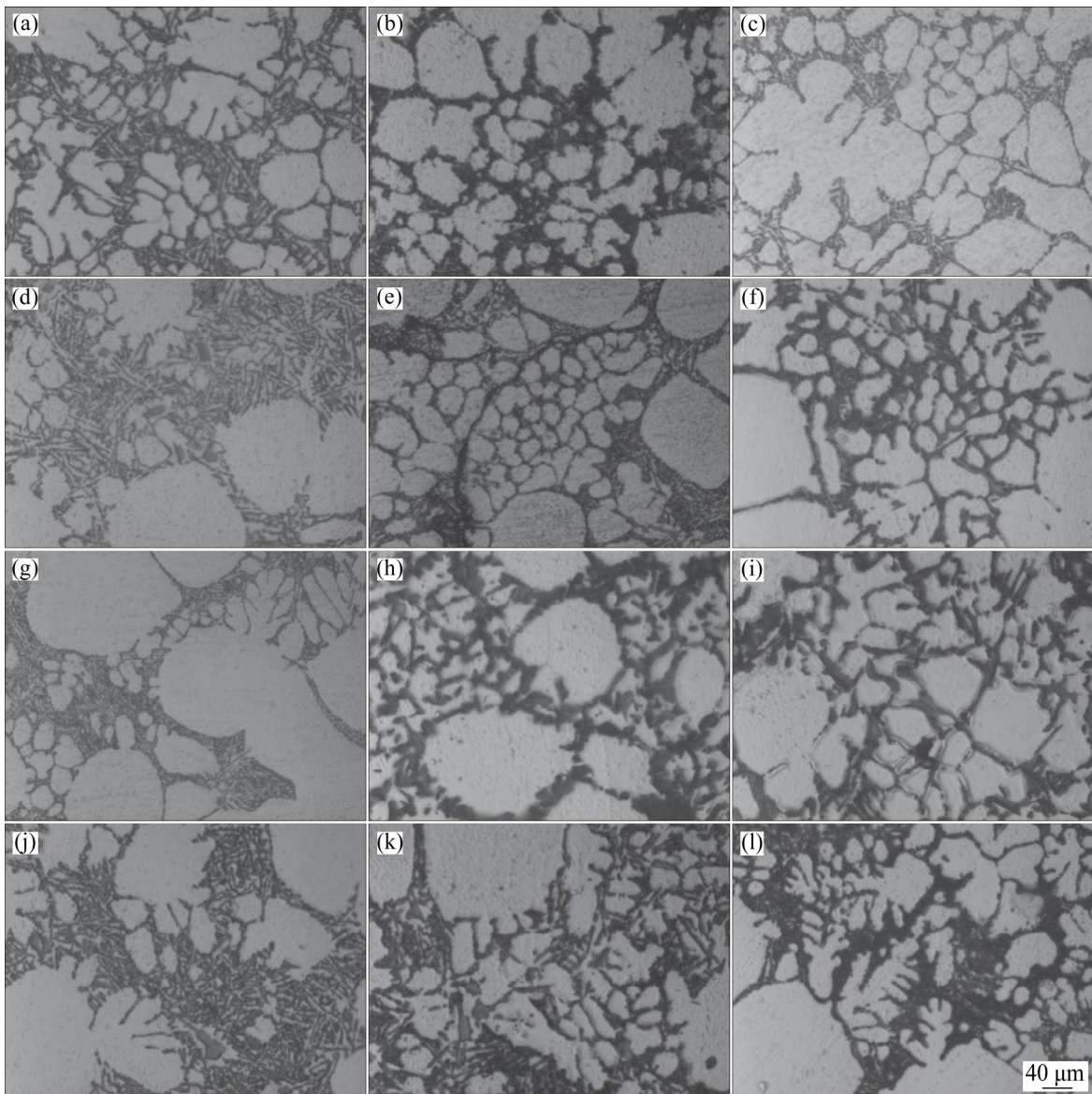


Fig. 9 Water-quenched microstructures of secondary solidification after isothermal holding for different time at different temperatures: (a, d, g, j) Holding at 590 °C for 0, 3, 5 and 10 min, respectively; (b, e, h, k) Holding at 600 °C for 0, 3, 5 and 10 min, respectively; (c, f, i, l) Holding at 610 °C for 0, 3, 5 and 10 min, respectively

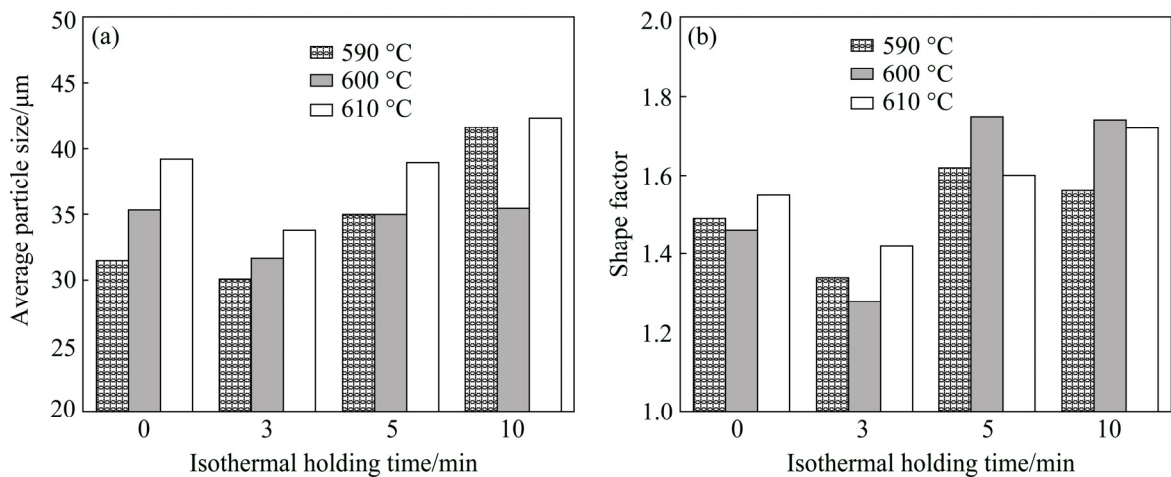


Fig. 10 Effects of isothermal holding time and temperature on average particle size (a) and shape factor (b) of secondary particles

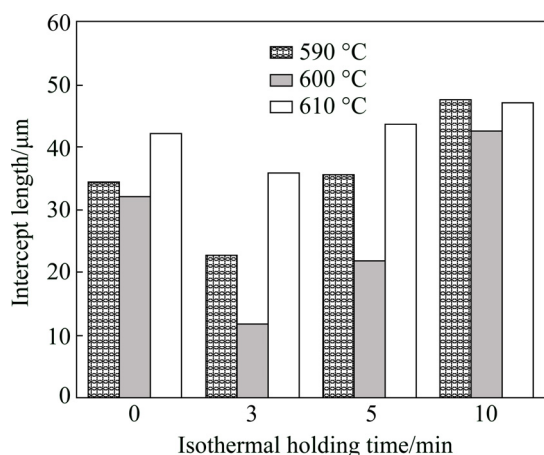


Fig. 11 Change of attached secondary particle size with isothermal holding time

the thermal field and concentration field of the remaining liquid is aggravated due to the increase of the merging phenomenon of the primary particles. Hence, the solidification condition is similar to the conventional casting. As a result, the coarse dendrites are formed in the water-quenched microstructures of the remaining liquid phase (Figs. 9(k) and (l)).

When the isothermal holding temperature of the slurry is 600 °C, the growth rate of the primary particles is the fastest, leading to the fastest solute diffusion, in other words, the time to reach equilibrium is the shortest. Therefore, the morphology of primary particles is the roundest when the slurry is isothermally held at 600 °C for 3 min. Meanwhile, when the isothermal holding time is 5 min, it can be seen that the shape factor of secondary

particles at 600 °C is the largest, indicating that the effect of the remaining liquid instability caused by the merging phenomenon among primary particles on water-quenched microstructures of the secondary particles is the most prominent at 600 °C. During the isothermal holding process from 5 to 10 min, the change of the attached particle size at 600 °C is the fastest (the largest slope as shown in Fig. 11), indicating that the diffusion rate at 600 °C is the fastest, which can further prove the correctness of the data obtained in Table 5.

3.4 Effects of isothermal holding temperature on secondary particles and eutectic structures

Figure 12 shows the water-quenched microstructures of the A356 aluminum alloy semisolid slurry after holding for 3 min. It can be seen that the amount of the secondary particles is the least while the area of eutectic region is the most when the isothermal holding temperature is 590 °C (Figs. 12(a)–(c)). The eutectic silicon morphologies at different holding temperatures are shown in Figs. 12(d)–(f). It can be seen that the morphologies of the eutectic silicon are all needle-like and blocky, but the eutectic structures are gradually compact with the increase of isothermal holding temperatures.

It is well known that the solid fraction of the semisolid slurry is closely related to the temperature. On the basis of Pandat (a thermodynamic calculation software), theoretically, the solid fraction of the A356 aluminum alloy at 610, 600 and 590 °C are 11%, 27% and 38.5%, respectively. According to the conservation of mass [30], the content of the remaining liquid phase,

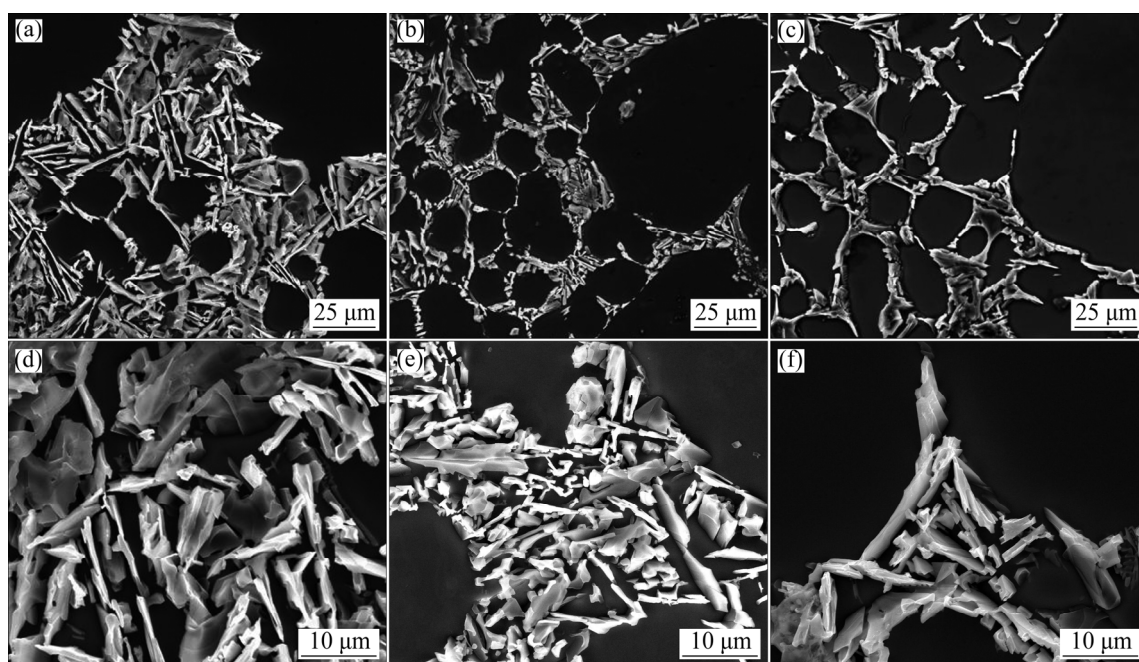


Fig. 12 Water-quenched microstructures of A356 aluminum alloy semisolid slurry after holding for 3 min: (a–c) Secondary particles at 590, 600 and 610 °C, respectively; (d–f) Eutectic structures at 590, 600 and 610 °C, respectively

C_1 , can be expressed as

$$C_1 = \frac{C_0 - C_s f}{1 - f} \quad (3)$$

where C_0 is the original content of the alloy, f is the solid fraction and C_s is the composition of the solid phase. The solute concentrations of the remaining liquid are calculated to be 7.80, 9.28 and 10.70, respectively, indicating that the compositions of the remaining liquid phase are deviated to the eutectic composition (12.6%) with the decrease of processing temperatures (isothermal holding temperatures). The changes of the solid fraction with temperature during the solidification of the original alloy and the remaining liquid of the three processing temperatures are shown in Fig. 13. The process of primary particles precipitating from liquid phase and their ripening can be regarded as the equilibrium solidification, while the solidification of remaining liquid phase is non-equilibrium solidification [31]. When the processing temperatures decrease from 615 to 590 °C, the solid fraction decreases gradually during the liquid phase solidification to eutectic temperature. Therefore, the amount of the secondary particles crystallized in the remaining liquid phase decreases with the decrease of the processing temperature. Hence, the limit effects of the secondary particles on the eutectic reaction gradually decrease. Moreover, the lower the processing temperature is, the larger the range of eutectic reaction to final solidification is, as a result, the more complete the eutectic reaction is. Together with the limit effects of secondary particles on the eutectic reaction regions, the eutectic structures are gradually compact with the decrease of the processing temperatures.

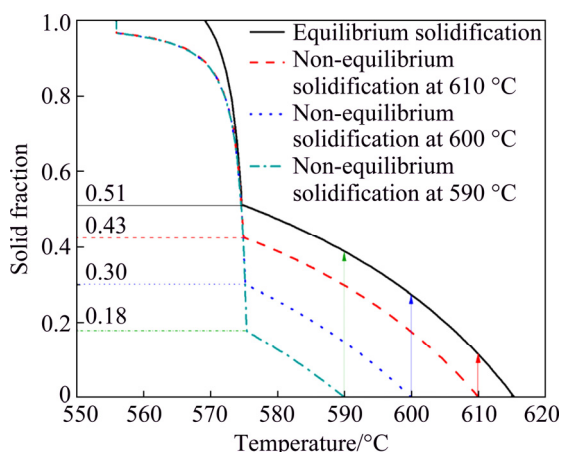


Fig. 13 Changes of solid fraction with temperature during solidification of original alloy and remaining liquid of three processing temperatures

4 Conclusions

1) The melt treatment temperature has large effect

on the final semisolid microstructure of the A356 aluminum alloy when the semisolid slurry is prepared by self-inoculation method. The semisolid slurry which is suitable for the rheological forming can be prepared when the melt treatment temperature is in the proper temperature range (680–690 °C).

2) The growth rate of the primary particles in the isothermal holding process conforms to the dynamic equation of $D_t^3 - D_0^3 = Kt$, and the coarsening rate of the primary particles at 600 °C is the fastest. The merging phenomena are gradually serious with the increase of isothermal holding time.

3) The secondary solidification microstructures are obviously different when the slurry undergoes different holding time. The secondary particles are the smallest and roundest when the isothermal holding time is 3 min. The size of the attached secondary particles is the smallest when the slurry is isothermally held at 600 °C for 3 min.

4) The amount of secondary particles gradually increases with the increase of isothermal holding temperature, which makes the eutectic reaction zones restricted. As a result, the final solidified eutectic structures are gradually compact.

References

- [1] Department of Engineering and Materials Science of the National Natural Science Foundation of China. Development planning reports of mechanical and manufacturing science[M]. Beijing: Science Press, 2011: 189–219. (in Chinese)
- [2] FLEMINGS M C. Behavior of metal alloys in the semi-solid state [J]. Metallurgical and Materials Transactions B, 1991, 22(5): 957–981.
- [3] LUO Shou-jing, JIANG Yong-zheng, LI Yuan-fa, SHAN Wei-wei. Recognition of semi-solid metal forming technologies [J]. Special Casting and Nonferrous Alloy, 2012, 32(7): 603–607. (in Chinese)
- [4] ESKIN D G, KATGERMAN S L. Mechanical properties in the semi-solid state and hot tearing of aluminum alloys [J]. Progress in Materials Science, 2004, 49(5): 629–711.
- [5] XU Jun, ZHANG Zhi-feng. Research progress of semisolid processing technology [J]. Journal of Harbin University of Science and Technology, 2013, 18(2): 1–6. (in Chinese)
- [6] ZHAO Jun-wen, WU Shu-sen. Microstructure and mechanical properties of rheo-diecasted A390 alloy [J]. Transactions of Nonferrous Metals Society of China, 2010, 20(S3): s754–s757.
- [7] FAN Z, FANG X, JI S. Microstructure and mechanical properties of rheo-diecast (RDC) aluminum alloys [J]. Materials Science and Engineering A, 2005, 412(1–2): 298–306.
- [8] MAHATHANINWONGA N, PLOOKPHOL T, WANNASINA J, WISUTMETHANGOON S. T6 heat treatment of rheocasting 7075 Al alloy [J]. Materials Science and Engineering A, 2012, 532(1): 91–99.
- [9] ZHU Wen-zhi, MAO Wei-min, TU Qin. Preparation of semi-solid 7075 aluminum alloy slurry by serpentine pouring channel [J]. Transactions of Nonferrous Metals Society of China, 2014, 24(4): 954–960.
- [10] GUAN Ren-guo, CAO Fu-rong, ZHAO Zhan-yong, HUANG Hong-qian, ZHANG Qiu-sheng, WANG Chao. Effects of wavelike sloping plate rheocasting and spheroidisation on microstructures and properties of Al–18%Si–5%Fe alloy [J]. The Chinese Journal of

- Nonferrous Metals, 2011, 21(9): 2084–2090. (in Chinese)
- [11] MARTINEZ R A, FLEMINGS M C. Evolution of particle morphology in semisolid processing [J]. Metallurgical and Materials Transactions A, 2005, 36(8): 2205–2210.
- [12] APELIAN D, FINDON M, PAN Q Y. Low cost and energy efficient methods for the manufacture of semi-solid (SSM) feedstock [J]. Die Casting Engineer, 2004, 48(1): 22–28.
- [13] KAUDMANN H, MUNDI A, POTZINGER R, UGGOWIRZER P J. An update on the new rheocasting-development work for Al and Mg alloys [J]. Die Casting Engineer, 2002, 46(4): 16–19.
- [14] MIDSON S P. Rheocasting processes for semi-solid casting of aluminum alloy [J]. Die Casting Engineer, 2006, 50(1): 48–51.
- [15] LI Ming, LI Yuan-dong, HUANG Xiao-feng, MA Ying, GUAN Ren-guo. Secondary solidification behavior of A356 aluminum alloy prepared by the self-inoculation method [J]. Metals, 2017, 7(7): 233–251.
- [16] HITCHCOCK M, WANG Y, FAN Z. Secondary solidification behaviour of the Al–Si–Mg alloy prepared by the rheo-diecasting process [J]. Acta Materialia, 2007, 55(5): 1589–1598.
- [17] JI S, DAS A, FAN Z. Solidification behavior of the remnant liquid in the sheared semisolid slurry of Sn–15wt%Pb alloy [J]. Scripta Materialia, 2002, 46(3): 205–210.
- [18] JI S, FAN Z. Extruded microstructure of Zn–5wt%Al eutectic alloy processed by twin screw extrusion [J]. Materials Science and Technology, 2012, 28(11): 1287–1294.
- [19] REISI M, NIROUMAND B. Growth of primary particles during secondary cooling of a rheocast alloy [J]. Journal of Alloys and Compounds, 2009, 475(1–3): 643–647.
- [20] ZANLER S, ERSHOV A, RACK A, GARCIA-MORENO F, BAUMBACH T, BANHART J. Particle and liquid motion in semi-solid aluminium alloys: A quantitative in situ microradiography study [J]. Acta Materialia, 2013, 61(4): 1244–1253.
- [21] GUAN Ren-guo, CHEN Li-qing, LI Jiang-ping, WANG Fu-xing. Dynamical solidification behaviors and metal flow during continuous semisolid extrusion process of AZ31 alloy [J]. Journal of Materials Science and Technology, 2009, 25(3): 395–400.
- [22] ZHAO Zhan-yong, GUAN Ren-guo, WANG Xiang, LIU Chun-ming. Microstructure formation mechanism during a novel semisolid rheo-rolling process of AZ91 magnesium alloy [J]. Acta Metallurgica Sinica (English Letters), 2013, 26(4): 447–454.
- [23] CHEN Zhong-wei, ZHANG Hai-fang, LEI Yi-min. Secondary solidification behaviour of AA8006 alloy prepared by suction casting [J]. Journal of Materials Science and Technology, 2011, 27(9): 769–775.
- [24] LI Chun, LI Yuan-dong, MA Ying, CHEN Ti-jun, WU Hui-hui, LI Yan-lei. Effects of self-inoculation technological parameters on semi-solid microstructure of ZA96 magnesium alloy and interactive nature [J]. The Chinese Journal of Nonferrous Metals, 2013, 23(3): 599–609. (in Chinese)
- [25] LI Chun, LI Yuan-dong, MA Ying, CHEN Ti-jun, WU Hui-hui, LI Yan-lei. Role of melt processing in preparation of Mg₉Zn₂Al magnesium alloy semisolid slurry [J]. The Chinese Journal of Nonferrous Metals, 2012, 22(6): 1536–1545. (in Chinese)
- [26] WANG Jian-zhong. The research of treating technology with electro-pulse modification and the hypothesis of liquid metal cluster structure [D]. Beijing: University of Science and Technology Beijing, 1998. (in Chinese)
- [27] WANG Guang-hou. Cluster physics [M]. Shanghai: Shanghai Science and Technology Press, 2003. (in Chinese)
- [28] DEEPAK K S, MIHIRA A, MANDAI A, CHAKRABORTY M. Coarsening kinetics of semi-solid A356–5wt%TiB₂ in situ composite [J]. Transactions of the Indian Institute of Metals, 2015, 68(6): 1075–1080.
- [29] VOORHEES P W, HARDY S C. Ostwald ripening in a system with a high volume fraction of coarsening phase [J]. Metallurgical and Materials Transactions A, 1988, 19(11): 2713–2721.
- [30] YANG Wei, LIU Feng, WANG Hai-feng, LU Yi-ping, YANG Gen-cang. Non-equilibrium transformation kinetics and primary grain size distribution in the rapid solidification of Fe–B hypereutectic alloy [J]. Journal of Alloys and Compounds, 2011, 509(6): 2903–2908.
- [31] GUO Hong-min, WEN Fei-ma, YANG Xiang-jie, JIN Hua-lan, ZHANG Ai-sheng. Thermodynamic analysis of processability of Mg–Al–Zn–Mn alloys for rheocasting [J]. Materials Science and Technology, 2015, 31(15): 1903–1909.

熔体处理温度及保温参数对 A356 铝合金半固态浆料水淬组织的影响

李明¹, 李元东^{1,2}, 毕广利^{1,2}, 黄晓锋^{1,2}, 陈体军^{1,2}, 马颖^{1,2}

1. 兰州理工大学 省部共建有色金属先进加工与再利用国家重点实验室, 兰州 730050;

2. 兰州理工大学 有色金属合金省部共建教育部重点实验室, 兰州 730050

摘要: 采用自孕育法制备 A356 铝合金半固态浆料, 研究熔体处理温度及保温参数对 A356 铝合金半固态浆料水淬组织的影响, 并分析剩余液相的二次凝固行为。结果表明: 熔体处理温度对最终半固态组织影响较为显著。当熔体温度在 680–690 °C 之间时, 可以制备出适合流变成形的半固态浆料。在等温保温过程中初生颗粒的生长速率符合 $D_t^3 - D_0^3 = Kt$ 动力学方程, 且当保温温度为 600 °C 时初生颗粒的粗化速率最快。此外, 等温保温时间对二次凝固组织的影响较明显。保温 3 min 时浆料水淬组织中的二次颗粒最为细小、圆整。随保温温度的升高, 二次颗粒数目逐渐增多。因此, 共晶反应被限制在很小的晶间区域内, 使最终凝固的共晶组织排列较为紧密。

关键词: 铝合金; 半固态; 自孕育法; 二次凝固; 初生颗粒; 共晶组织

(Edited by Wei-ping CHEN)